Journal of King Saud University – Science 35 (2023) 102627

HOSTED BY

Contents lists available at ScienceDirect

Journal of King Saud University – Science

journal homepage: www.sciencedirect.com

Original article

Comparative efficacy of epigallocatechin gallate and its nano-formulation in prostate cancer 3D spheroids model

Read F. Alserihi [a], Mohammed Razeeth Shait Mohammed [b], Mohammed Kaleem [b,c], Mohammad Imran Khan [b], Mario Sechi [d], Torki A. Zughaibi [a,e], Shams Tabrez [a,e,*]

[a] Department of Medical Laboratory Sciences, Faculty of Applied Medical Sciences, King Abdulaziz University, Jeddah, Saudi Arabia
[b] Department of Biochemistry, Faculty of Science, King Abdulaziz University, Jeddah, Saudi Arabia
[c] Department of Pharmacology, Dadasaheb Balpande College of Pharmacy, Nagpur, Maharashtra, India
[d] Department of Chemistry and Pharmacy, Laboratory of Drug Design and Nanomedicine, University of Sassari, 07100 Sassari, Italy
[e] King Fahd Medical Research Center, King Abdulaziz University, Jeddah, Saudi Arabia

ARTICLE INFO

Article history:
Received 20 December 2022
Revised 23 January 2023
Accepted 26 February 2023
Available online 2 March 2023

Keywords:
3D spheroids
Anticancer
Epigallocatechin gallate
Nanoparticles
Polyphenols
Prostate cancer

ABSTRACT

Background: Prostate cancer (PCa) remains one of the clinically relevant pathologies that needs pragmatic and effective treatment approaches. The current study aimed to evaluate the anticancer potential of epigallocatechin gallate (EGCG) and EGCG-loaded nanoparticles (EGCG NP) for the treatment of prostate cancer in *in-vitro* 3D spheroid model.

Methods: The EGCG NPs was synthesized by using polymeric method as reported in our previous study. A 3D spheroid assay was conducted using human prostate specific cell lines (PC3 and 22Rv1) cultured on poly-HEMA-covered plates at different time points. Once formed, the spheroids were treated with either EGCG alone or with EGCG NPs continuously for 6 days. Simultaneously, specific controls were also taken for comparison purpose. CellROX dye was used to quantitate the formation of reactive oxygen species (ROS) in response to EGCG and EGCG NPs to 22Rv1 and PC3, 3D spheroids. The treated spheroids were also evaluated to measure modulation in mitochondrial membrane potential and the quantification of apoptotic and live cells using a flow cytometer.

Results: The spheroid sizes of both studied cell lines were found to be significantly ($p < 0.05$) reduced after the treatment with EGCG and its nanoformulation. The significant increase in ROS formation was observed in PC3 cells in response to EGCG and EGCG-NPs treatment. However, no significant change in ROS formation was observed in 22Rv1 cells. Similarly, both compounds (EGCG and EGCG NPs) did not show any significant changes in mitochondrial membrane potential in 22Rv1 and PC3 spheroids. Interestingly, EGCG treatment showed a significant change between live and apoptotic cells in both 22Rv1 and PC3 spheroids but its nanoformulation didn't show any significant change in the number of apoptotic and live cells. Our study observed a significant anticancer potential of EGCG and EGCG NPs at clinically relevant doses highlighting the possible advantage of 3D spheroid model specifically in our studied cancer cells. However, further preclinical *in vivo* studies are recommended in a suitable model to decipher our *in vitro* data and exploit EGCG and EGCG NPs against prostate cancer.

Conclusion: Our results indicate the anticancer efficacy of EGCG and EGCG NPs in 3D spheroids of PCa cell lines.

1. Introduction

Prostate cancer (PCa) is one of the clinically relevant pathologies, has progressively increased its global prevalence over the past decade (Li et al., 2022). It is the most often diagnosed male cancer and the leading cause of cancer-associated mortality in males around the globe (Sung et al., 2021). In 2021, it was estimated that 26% of newly found non-cutaneous cancer will be because of PCa resulting in total 11% cancer-related deaths in the USA

* Corresponding author at: King Fahd Medical Research Center, King Abdulaziz University, P. O. Box 80216, Jeddah 21589, Saudi Arabia.
E-mail address: shamstabrez1@gmail.com (S. Tabrez).

Peer review under responsibility of King Saud University.

Production and hosting by Elsevier

https://doi.org/10.1016/j.jksus.2023.102627
1018-3647/

(Picot et al., 2022). Over the past few years, the incidence of metastatic PCa has increased in all races and age groups, ultimately affecting the survival rate (Sayegh et al., 2022). The existing curative and noncurative therapeutic options of PCa, such as surgery, radiation therapy, hormonal therapy, and chemotherapy are overburdened by various side effects, that include limited clinical efficacy, high cost, and low patient acceptance (Li et al., 2022). In addition, the chemotherapeutic option against PCa is limited due to poor solubility, toxicity, lack of target specificity, nonspecific cell damage and drug resistance (El-Didamony et al., 2022). Despite of the intriguing therapeutic options, the search for pragmatic and more effective treatments modalities that could mitigate abovementioned undesirable effects are need of the hour.

The surge of naturally derived chemotherapeutic agents provide hopes for effective chemotherapy against PCa (El-Didamony et al., 2022). The phytochemicals have been explored as the cornerstone of highly efficient, well-tolerated, safe, and economical approaches in multifaceted PCa prevention and management (Mazurakova et al., 2022). Based on our earlier research, we also proposed some bioactive molecules and their nanoformulations as potential anticancer agents (Jabir et al., 2012, 2018a; Oves et al., 2018; Tabrez et al., 2013).

Epigallocatechin gallate (EGCG), the primary flavonoid in green tea, has shown significant efficacy in the treatment of cancer due to its considerable therapeutic properties, such as safety, affordability, and bioavailability (Jabir et al., 2018b). Several studies suggested that EGCG may inhibit carcinogenesis *via* anti-matrix metalloproteinase and anti-angiogenesis activities, blocking key signal transduction pathways and activating redox-sensitive transcription factors (Liu et al., 2019; Ferrari et al., 2022). The EGCG mediated therapeutic approach needs further improvements in terms of stability, specificity, low absorption, bioavailability, and safety (Dai et al., 2020). In this context, nanotechnology-based approaches have shown significant improvement in anti-cancer potential of EGCG against various cancers (Ahmad et al., 2019; Alserihi et al., 2022). Polymeric nanoparticle is one of the most effective ways to circumvent the delivery and protect the molecules against undesirable circumstances (Ahmad et al., 2020; Ahmad et al., 2021). Recently, we reported the enhanced antitumor efficacy of EGCG loaded folate receptor-targeted nanoparticles to PCa cells (Alserihi et al., 2022). The current study aimed to assess the therapeutic potential EGCG and EGCG-NPs against PCa cancer cell lines using 3D spheroid model. The purpose of choosing 3D cell culture was to mimic the *in vivo* environment so that we can achieve a robust and more reliable data (Choi et al., 2021).

2. Materials and methods

2.1. Synthesis and characterization of EGCG-NPs

The polymeric synthesis and characterization of EGCG-NPs using a modified polymeric nanoprecipitation method was described earlier in detail (Alserihi et al., 2022). After dilution of samples with Milli-Q water, NPs' mean diameter and polydispersity index (PDI) were evaluated using photon correlation spectroscopy (Zetasizer Nano ZS, Malvern Instruments, UK) at 25 °C and at a scattering angle of 90°.

2.2. Culture of cells

22Rv1 and PC3, prostate tumorigenic cell lines were procured from ATCC (Manassas, VA, USA). Both cell lines were cultivated in an appropriate culture medium [RPMI-1640 and DMEM-high glucose], which included 10% fetal bovine serum and 1% penicillin.

2.3. 3D spheroid assay

For the induction of 3D spheroid, we grew both cancer cell lines on poly-HEMA-coated plates for different time points. Once formed, the spheroids were treated with either EGCG or with EGCG-NPs, continuously for 6 days. Simultaneously, specific control was also taken for comparison purpose. In addition, an empty NPs without EGCG was used as control to compare the effect of EGCG NPs. Every two days, new media was added to replace the spent media. Nikon's inverted light microscope was used to take the spheroids' photos, which were then examined for size using the image J software (https://image j.net/Invasion assay).

2.4. Measurement of reactive oxygen species in spheroids

Reactive oxygen species (ROS) production in spheroids was measured using the CellROX dye (Life Technologies, Carlsbad, CA, USA). Both cell lines were plated in six-well poly-HEMA-coated plates and continuously exposed to either EGCG, or EGCG NP for 6 days to quantify ROS. CellROX (500 nM) was added when the time point was reached, and it was then incubated at 37 °C with 5% CO_2 for 60 min. Following the incubation, the samples were examined at flow cytometer utilizing CellROX® Green at 488 nm excitation.

2.5. Measurement of mitochondrial membrane potential in spheroids

The spheroids were continuously incubated for 6 days with either control and EGCG or empty NP and EGCG NP for the mitochondrial membrane potential (MMP) measurement (Mittal et al., 2017). A flow cytometer (Guava easyCyte™ Luminex) equipped with a 485 nm excitation filter and a 590 nm emission filter was used to examine the treated cells for red and green fluorescence.

2.6. Live/dead assay in spheroids

Spheroids were continually exposed to EGCG, and EGCG NP for 6 days as part of this test. Propidium iodide (PI) dye in culture media was added to the spheroids once the time point was complete, and they were then washed with 1X PBS and incubated for 10 min at 37 °C. A flow cytometer (Guava easyCyteTM Luminex) was then used to examine the cells for red fluorescence.

2.7. Statistical analysis

The GraphPad Prism 8.0 software was used to conduct a one-way analysis of variance for various groups to find differences between the control and treated groups (GraphPad Software, La Jolla, CA, USA). All the experiments were performed in triplicate and results are reported as mean ± SD. $p < 0.05$ were deemed statistically significant.

3. Results and discussion

The NPs' particle sizes suggests that the addition of EGCG, did not resulted a significant increase in size when compared to the corresponding free counterparts (Table 1). The 0.12 PDI values that defined the NP dispersions showed a narrow and unimodal distribution, which is typical behavior of monodispersed systems. The encapsulation efficiency of EGCG-NP was found to be 44%, indicating a moderate affinity of the polymeric blend with the EGCG molecules in terms of drug entrapment efficiencies. Additionally, the yields of production were found to be in between 67% and 73%.

Table 1
Average diameter, polydispersity index (PDI), percentage of encapsulation efficiency (EE %), EGCG loading content (DLC %) and yield of production (YP %) of formulated NPs. Data are mean ± SD, n = 3.

Batch	Mean diameter (nm)	PDI	EE (%)	DCL (%)	YP (%)
Ø-NP	110.21 ± 4.24	0.115 ± 0.01	–	–	73.50 ± 4.95
EGCG-NP	123.31 ± 7.42	0.121 ± 0.03	44.15 ± 2.48	2.21 ± 0.12	67.82 ± 5.76

Anticancer screening of compounds is mostly performed in conventional 2D cell cultures which often doesn't concur in animal model. Hence, 3D spheroid culture models are gaining interest lately because they mimics human tumor tissue conditions (Hundsberger et al., 2021). 3D culture methods typically use an extracellular matrix which imitate tissue key interactions including, cell-to-cell and cell-to-extracellular matrix interactions (Białkowska et al., 2020). In 3D culture, the cells grow, aggregate, and self-assemble in a 3D plane in an environment that prevents attachment to a flat surface, resulting in the formation of spheroid, resembling to *in vivo* tumors (Lazzari et al., 2017). The advantages of 3D spheroids include the possibility of screening a large number of molecules, reducing high cost and ethical issues associated with animal usage (Pinto et al., 2020). In the present study, we used 3D model to assess the impact of both EGCG and EGCG NP treatment in PCa cell lines, namely, 22Rv1 and PC3.

Contemplating the earlier studies, we speculated the diverse therapeutic functions of EGCG in different PCa cell lines could be mediated by androgen sensitivity (Bosutti et al., 2016, Russo et al., 2020). Hence, we choose two different PCa cell lines viz. 22RV1 (androgen-responsive) and PC3 (androgen-nonresponsive) for comparison.

3.1. EGCG and EGCG NPs treatment reduces spheroid size of PCa cell lines

Spheroid size is one of the crucial aspects to assess the efficacy of the test compounds. The spheroid formation was accomplished by seeding cell suspensions into ultra-low poly-HEMA-coated plates. The microscopic examination of these spheroids showed different morphometric characteristics of 22Rv1 and PC3 cells. The treatment of 3D spheroid with the EGCG and EGCG NPs resulted visible changes in their morphology during the treatment period of 6 days. The treatment of EGCG and EGCG NPs showed significant reduction in spheroid size compared to that of control (Fig. 1 and Fig. 2).

As shown in Fig. 1 (a and b upper panel), detachment of both 22Rv1 and PC3 cells resulted in gradual increase of spheroid size in controls, i.e., from 271.5 mm^3 on the second day to 569.3 mm^3 on the sixth day in 22Rv1 cells and from 243.5 mm^3 on the second day to 360.7 mm^3 on the sixth day in PC3 cells. EGCG treatment significantly reduces the spheroid sizes on 6th days from 569.3 to 107.9 mm^3 in the 22Rv1 cell line (Fig. 1a, lower panel). Furthermore, we observed a similar decrease in the spheroid size on 6th day from 360.7 to 42.7 mm^3 in the PC3 cells (Fig. 1b, lower panel). Overall, the data clearly showed that the treatment of EGCG significantly attenuates spheroid size of 22Rv1 and PC3 cells.

Similarly, we also assessed the impact of EGCG NPs treatment on spheroids size by comparing with empty NPs in 22Rv1 and PC3 cells. As shown in Fig. 2 (a and b upper panel), detachment of both cell lines resulted in a gradual increase in spheroid size in the presence of empty NPs, i.e., from 193 mm^3 on the second day to 248.3 mm^3 on the sixth day in 22Rv1 cells and from 221.2 mm^3 on the second day to 348.7 mm^3 on the sixth day in PC3 cells. On the other hand, the treatment with EGCG NPs significantly reduces the spheroid sizes on 2nd and 6th days, corresponding to 193 to 95.7 mm^3 and 248.3 to 102 mm^3, respectively in the 22Rv1 cell line (Fig. 2a, lower panel). Albeit

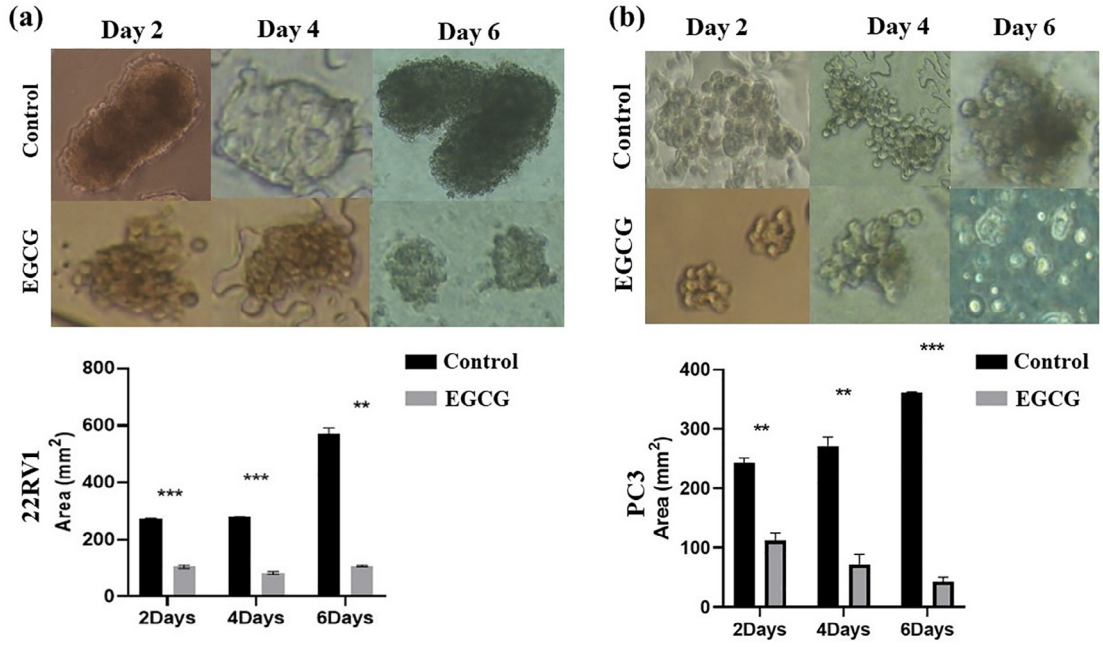

Fig. 1. Spheroid size decreased with EGCG treatment. Both (a) 22Rv1 and (b) PC3 underwent EGCG treatment for 2–6 days after completing full growth in poly-HEMA-coated plates forming 3D spheroids. Images were captured with a Nikon inverted light microscope, and size analysis was performed using the image J software (mean ± SEM). **P < 0.01, and ***P < 0.001. For size measurement, 100 spheroids in total were examined.

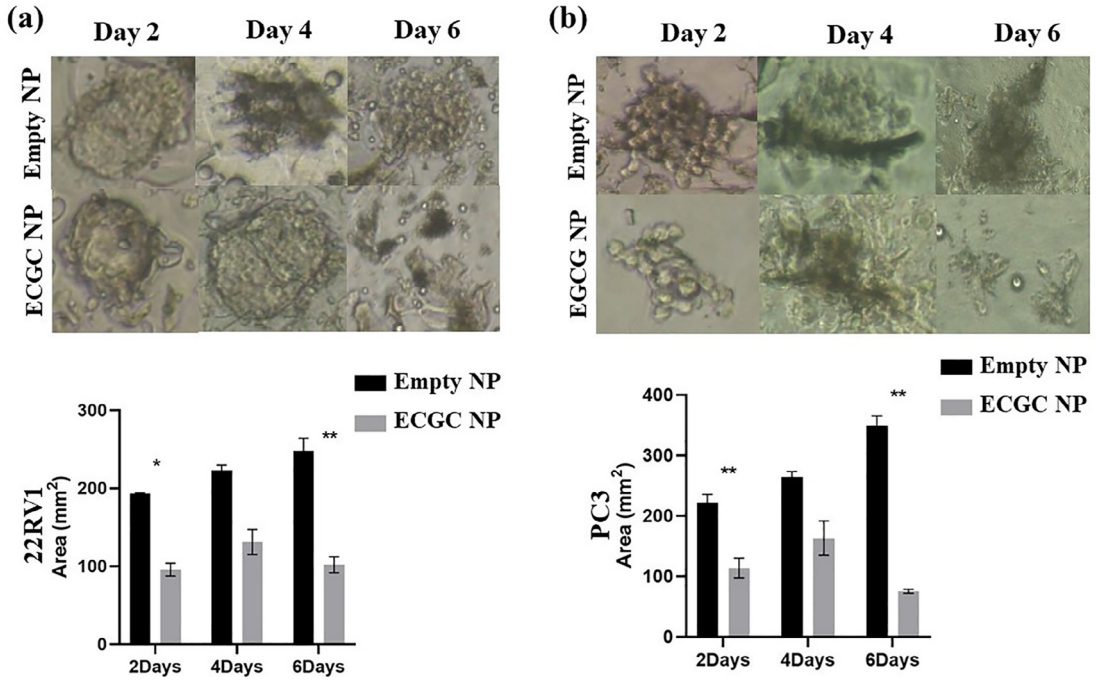

Fig. 2. Spheroid size is decreased by EGCG NPs treatment. In poly-HEMA-coated plates, (a) 22Rv1 and (b) PC3 were fully grown to form 3D spheroids. Pictures were acquired using a Nikon inverted light microscope at 40x magnification after the spheroids were treated for 2–6 days with empty nanoparticles or EGCG NPs. Using image J software, images were processed for size measurement (mean ± S.E.M.). *P < 0.05, and **P < 0.01. 100 spheroids in total were measured for size analysis.

there was a decrease in the spheroid size from 222.5 to 131.33 mm^3 on the 4th day in 22Rv1, the difference was not statistically significant. Furthermore, we observed a similar decline in the spheroid size on the second day from 221.2 to 114.2 mm^3 and 348.7 to 75.6 mm^3 on the sixth day (Fig. 2b, lower panel) in the PC3 cell line. Like 22Rv1, PC3 cells also showed a non-significant decrease in spheroid size on the 4th day of EGCG NP treatment from 264.5 to 163.5 mm^3. These data revealed that the treatment of EGCG NPs significantly attenuates spheroid formation of detached PCa cells.

Spheroid growth result in the formation of necrotic/hypoxic cores with the outside layer largely proliferative, the middle layer hypoxic, and the inner core necrotic (Sims et al., 2017). The efficacy of a drug/compound to penetrate a tumor depends heavily on the

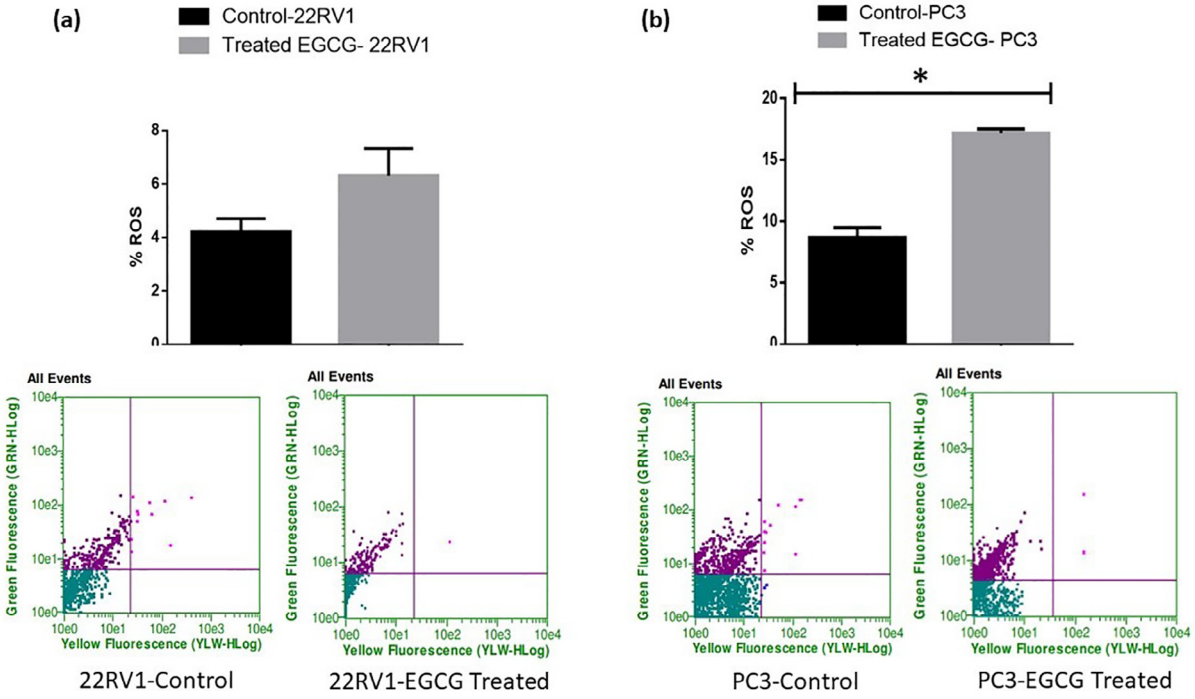

Fig. 3. EGCG fails to induce ROS in spheroids in 22Rv1 cells (a) and induces ROS in PC-3 cells (b). On poly-HEMA-coated plates, the cells were cultivated before treatment for six days with EGCG (6 μM). CellROX dye was applied to the spheroids at the end of time point and was incubated for 30 min in the dark. The manufacturer-provided standardized wavelength and the Guava Flow Cytometer was used to quantify fluorescent intensity. The values are presented as mean ± SEM (n = 6).

size of the tumor because larger tumors exhibit higher resistance, which is also seen in 3D tumor spheroid models (Perez et al., 2021). In the current study, we observed a dramatic decrease in the spheroid size as a result of both EGCG and EGCG NP treatment in 22Rv1 and PC3 cell lines. A comparatively higher reduction in spheroid size was noted in the PC3 cells after the treatment with EGCG and EGCG NPs. Previous studies suggested various anticancer mechanisms of EGCG and EGCG NPs, such as influence on cellular

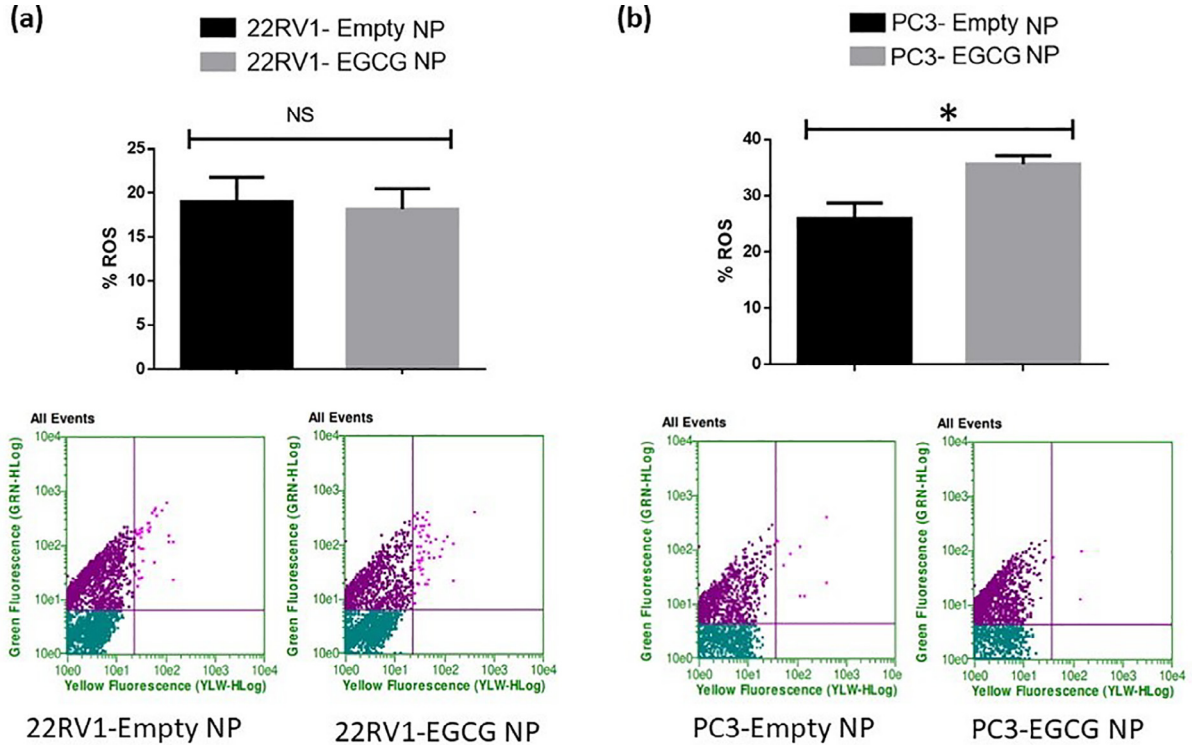

Fig. 4. EGCG NPs fails to induce ROS in spheroids 22Rv1 cells (a) and induces ROS in PC-3 cells (b). On poly-HEMA-coated plates, the cells were cultivated before being treated for six days with EGCG NPs (6 μM). CellROX dye was applied to the spheroids at the end of the time point and was incubated for 30 min in the dark. The manufacturer-provided standardized wavelength and the Guava Flow Cytometer was used to quantify fluorescent intensity. The values are presented as mean ± SEM (n = 6).

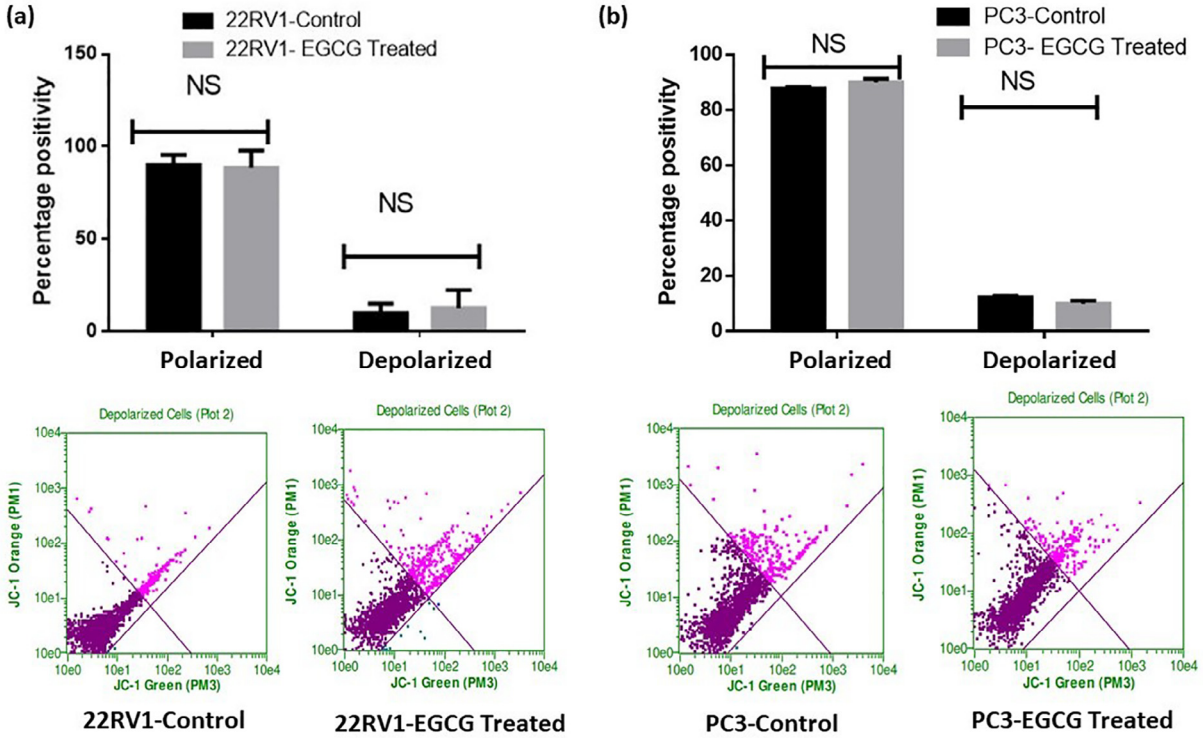

Fig. 5. EGCG fails to induce depolarization in PCa spheroids. The treated spheroids were mixed with JC-1 dye at the time point's end, and they were then incubated for 30 min at 37 °C. The manufacturer-provided standardized wavelength for the Guava Flow Cytometer was used to measure the fluorescent intensity. The values are shown as the mean ± SEM (n = 6).

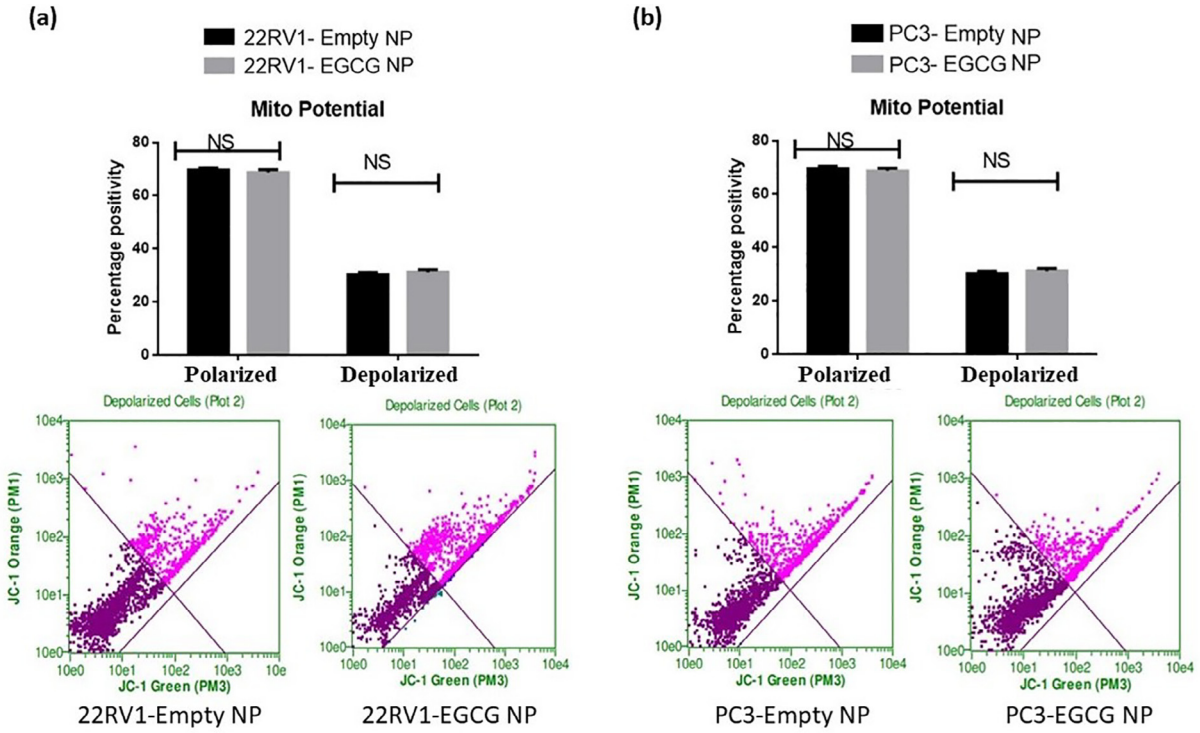

Fig. 6. EGCG NPs fails to induce depolarization in PCa spheroids. The treated spheroids were mixed with JC-1 dye at the time point's end, and they were then incubated for 30 min at 37 °C. The manufacturer-provided standardized wavelength for the Guava Flow Cytometer was used to measure the fluorescent intensity. The values are shown as the mean ± SEM (n = 6).

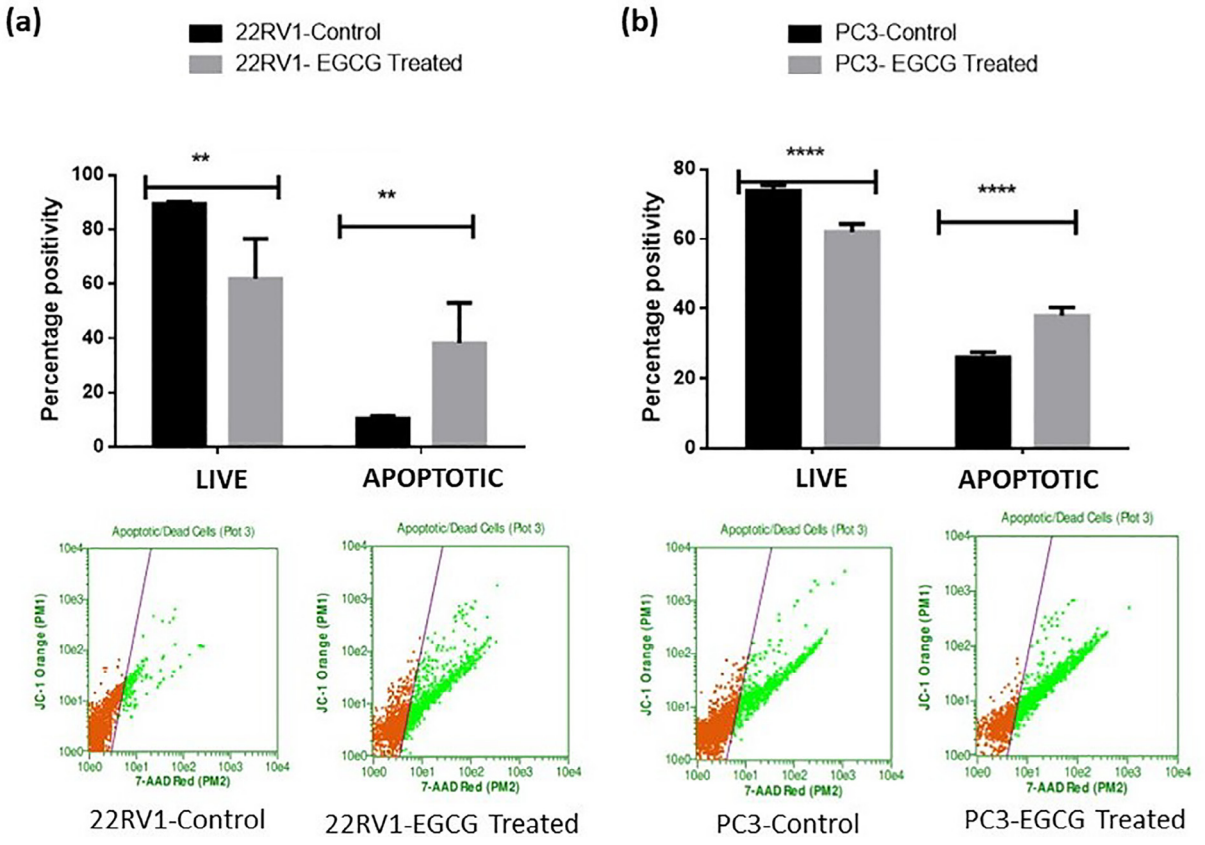

Fig. 7. EGCG induced apoptosis in PCa spheroids. The treated spheroids received PI dye at the end of the time point, and they were then incubated for 30 min at 37 °C. Using a Guava Flow Cytometer and a defined wavelength that the manufacturer provided, fluorescent intensity was assessed. The values are shown as the mean ± SEM (n = 6). **P < 0.01 and ***P < 0.001.

apoptosis, ROS generation, and inhibition of mutant p53 or tyrosine kinase (Cheng et al., 2020; Farooqi et al., 2020). Our results are concurrent with different studies that uses PLGA/lipid NPs loaded EGCG in 3D models (Hung et al., 2016; Sims et al., 2017; Michy et al., 2019). Sims et al. (2017) reported an increased penetration and distribution of PLGA-modified NPs in HeLa and SiHa spheroids (Sims et al., 2017). The PLGA-encapsulated EtNBS NPs deeply penetrated the 3D spheroid of gastrointestinal carcinoma's hypoxic and acidic cores, which are typically therapeutically resistant tumor regions (Hung et al., 2016). In ovarian spheroid cancer cells, verteporfin-encapsulated lipid nanocarriers effectively inhibited proliferation than free verteporfin (Michy et al., 2019). Similarly, biotin-conjugated pullulan acetate NPs has been noted for comparable anticancer activity in 3D culture and a xenograft hepatic tumor model (Chen et al., 2019).

3.2. EGCG and EGCG NPs treatment induce ROS in spheroids of PC3 not in 22Rv1

We assessed the impact of EGCG & EGCG NPs treatment on ROS production using flowcytometry by applying CellROX dye at the end of the sixth day in darkness for 30 min. The EGCG and EGCG NPs treatment fails to induce a statistically significant production of ROS in 22Rv1 spheroids compared to controls [Figs. 3 & 4 (a, upper and lower panels)]. However, EGCG and EGCG NPs treatment induces significant production of ROS in PC3 cells [Figs. 3 & 4 (b, upper and lower panels)].

These results indicate involvement of ROS-mediated mechanism(s) in PC3 cells for antitumorigenic effects of EGCG and EGCG NPs. Since, the elevated levels of ROS has been reported to trigger anticancer mechanisms, treating cancer cells with ROS stimulating agents may offer cancer-specific therapy (Gul et al., 2022). The expression of prostate specific membrane antigen (PSMA) have shown relationship with androgen signaling that could play an important clinical implications for PCa treatment (Batra et al., 2019). However, several studies reported that ROS are not an obligatory contributor to produce anticancer effects (Ivanova et al., 2016, Alserihi et al., 2022).

3.3. EGCG and EGCG NPs treatment fails to promote mitochondrial leakage in PCa cells

The spheroids of both 22Rv1 and PC3 cells treated with EGCG and EGCG NPs showed a non-significant association in mitochondrial depolarization as evident by JC-1 dye fluorescence (Figs. 5 & 6, upper and lower panels). The increase in depolarization and decrease in polarization of mitochondria membrane potential has been reported as important hallmarks of tumorigenesis (Porporato et al., 2018). These results pointed the possibility of mitochondrial independent mechanism of cytotoxicity and ROS production. Recently, Adamczuk et al. (2021) also reported a mitochondria-independent cytotoxic effect of leflunomide in RPMI-8226 multiple myeloma cell lines (Adamczuk et al., 2021). ROS are not only produced by mitochondria in living things, but also by NADPH oxidases, xanthine oxidase, oxidases of aldehydes, amino acids, and carbohydrates under specific conditions in a precise spatiotemporal manner (Lushchak 2016).

3.4. EGCG treatment promotes apoptosis in PCa cells

Fig. 7 (a, b), upper and lower panels show that there was a highly significant difference between 22Rv1 and PC3 spheroids

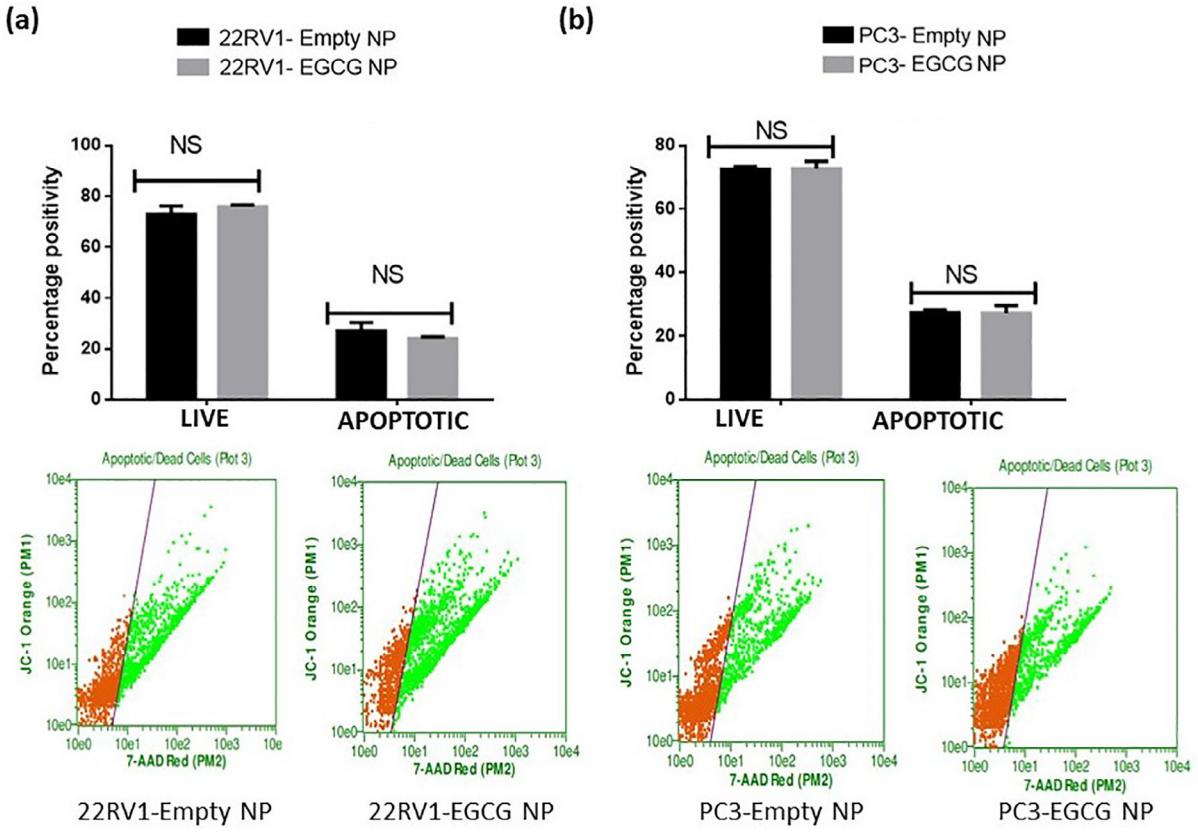

Fig. 8. EGCG NPs fails to induce apoptosis in PCa spheroids. The treated spheroids received PI dye at the end of the time point, and they were then incubated for 30 min at 37 °C. Using a Guava Flow Cytometer and a defined wavelength that the manufacturer provided, fluorescent intensity was assessed. The values are shown as the mean ± SEM (n = 6). **P < 0.01 and ***P < 0.001.

treated with EGCG in terms of the number of living and apoptotic cells. Moreover, 22Rv1 cells treated with EGCG showed an increase in apoptotic cells of almost 72% when compared to control. On the other hand, the number of apoptotic cells increased in PC3 spheroids treated with EGCG by 31% in comparison to control. These results were expected, as the EGCG has been reported to induce apoptosis in various cancer models (Zhao et al., 2021; Khiewkamrop et al., 2022). However, the EGCG NPs were failed to show a significant change in live and apoptotic cells in 22Rv1 and PC3 spheroids compared to empty NPs (Fig. 8).

4. Conclusion

Overall, our results indicate the anticancer efficacy of EGCG and EGCG NPs in 3D spheroids of PCa cell lines. The spheroid sizes of studied cell lines were significantly reduced after the treatment with EGCG and EGCG NPs. The EGCG and EGCG NPs induced ROS in PC3 cells but didn't induced in 22Rv1 cells possibly suggesting, no role of receptor mediated antigen i.e., PSMA. Surprisingly, we didn't observe any significant changes in mitochondrial membrane potential treated with EGCG or EGCG NP in 22Rv1 and PC3 spheroids. On the other hand, there was significant increase in apoptotic cells in EGCG treated groups. Overall, our results indicate a significant anticancer potential of EGCG alone. In addition, the nanoform version mostly showed better potential compared with EGCG alone. Further, preclinical *in vivo* studies and possible modulation in nanoform are recommended to verify our *in vitro* data and further enhance its potential for possible usage in clinics.

Declaration of Competing Interest

The authors declare that they have no known competing financial interests or personal relationships that could have appeared to influence the work reported in this paper.

Acknowledgments

The authors extend their appreciation to the Deputyship for Research & Innovation, Ministry of Education in Saudi Arabia for funding this research work through the project number 986.

Appendix A. Supplementary material

Supplementary data to this article can be found online at https://doi.org/10.1016/j.jksus.2023.102627.

References

Adamczuk, G., Humeniuk, E., Iwan, M., et al., 2021. The mitochondria-independent cytotoxic effect of leflunomide on RPMI-8226 multiple myeloma cell line. Molecules 26 (18), 5653. https://doi.org/10.3390/molecules26185653.

Ahmad, A., Khan, F., Mishra, R.K., et al., 2019. Precision cancer nanotherapy: evolving role of multifunctional nanoparticles for cancer active targeting. J. Med. Chem. 62 (23), 10475–10496. https://doi.org/10.1021/acs.jmedchem.9b00511.

Ahmad, A., Gupta, A., Ansari, M.M., et al., 2020. Hyperbranched polymer-functionalized magnetic nanoparticle-mediated hyperthermia and niclosamide bimodal therapy of colorectal cancer cells. ACS Biomater. Sci. Eng. 6 (2), 1102–1111. https://doi.org/10.1021/acsbiomaterials.9b01947.

Ahmad, A., Ansari, M.M., Verma, R.K., et al., 2021. Aminocellulose-grafted polymeric nanoparticles for selective targeting of CHEK2-deficient colorectal cancer. ACS Appl. Bio Mater. 4 (6), 5324–5335. https://doi.org/10.1021/acsabm.1c00437.

Alserihi, R.F., Mohammed, M.R.S., Kaleem, M., et al., 2022. Development of (−)-epigallocatechin-3-gallate-loaded folate receptor-targeted nanoparticles for prostate cancer treatment. Nanotechnol. Rev. 11 (1), 298–311. https://doi.org/10.1515/ntrev-2022-0013.

Batra, J.S., Pienta, K.J., Pomper, M.G. et al., 2019. Can the interplay between androgen signaling and PSMA expression be leveraged for theranostic applications? Transl. Androl. Urology. 0 (0) S263-S226S264. https://doi.org/10.21037/tau.2019.03.13.

Białkowska, K., Komorowski, P., Bryszewska, M., et al., 2020. Spheroids as a type of three-dimensional cell cultures-examples of methods of preparation and the most important application. Int. J. Mol. Sci. 21 (17), E6225. https://doi.org/10.3390/ijms21176225.

Bosutti, A., Zanconati, F., Grassi, G., et al., 2016. Epigenetic and miRNAs dysregulation in prostate cancer: the role of nutraceuticals. Anticancer Agents Med Chem. 16 (11), 1385–1402. https://doi.org/10.2174/1871520616666160425105257.

Chen, H., Wei, X., Chen, H., et al., 2019. The study of establishment of an in vivo tumor model by three-dimensional cells culture systems methods and evaluation of antitumor effect of biotin-conjugated pullulan acetate nanoparticles. Artif. Cells Nanomed. Biotechnol. 47 (1), 123–131. https://doi.org/10.1080/21691401.2018.1544142.

Cheng, Z., Zhang, Z., Han, Y., et al., 2020. A review on anti-cancer effect of green tea catechins. J. Funct. Foods 74, 104172. https://doi.org/10.1016/j.jff.2020.104172.

Choi, J.W., Bae, S.-H., Kim, I.Y. et al., 2021. Testing in vitro toxicity of nanoparticles in 3D cell culture with various extracellular matrix scaffold. https://doi.org/10.1101/2021.03.18.436024.

Dai, W., Ruan, C., Zhang, Y., et al., 2020. Bioavailability enhancement of EGCG by structural modification and nano-delivery: A review. J. Funct. Foods 65,. https://doi.org/10.1016/j.jff.2019.103732 103732.

El-Didamony, S.E., Amer, R.I., El-Osaily, G.H., 2022. Formulation, characterization and cellular toxicity assessment of a novel bee-venom microsphere in prostate cancer treatment. Sci. Rep. 12 (1), 13213. https://doi.org/10.1038/s41598-022-17391-w.

Farooqi, A.A., Pinheiro, M., Granja, A., et al., 2020. EGCG mediated targeting of deregulated signaling pathways and non-coding RNAs in different cancers: focus on JAK/STAT, Wnt/β-catenin, TGF/SMAD, NOTCH, SHH/GLI, and TRAIL mediated signaling pathways. Cancers 12 (4), 951. https://doi.org/10.3390/cancers12040951.

Ferrari, E., Bettuzzi, S., Naponelli, V., 2022. The potential of epigallocatechin gallate (EGCG) in targeting autophagy for cancer treatment: A narrative review. Int. J. Mol. Sci. 23 (11), 6075. https://doi.org/10.3390/ijms23116075.

Gul, S., Hassan, S.H., Maryam, A., et al., 2022. Chemopreventive and chemosensitizing effects of green tea: an evidence-based review. PJZ. 54 (5). https://doi.org/10.17582/journal.pjz/20191021131001.

Hundsberger, H., Stierschneider, A., Sarne, V., et al., 2021. Concentration-dependent pro- and antitumor activities of quercetin in human melanoma spheroids: comparative analysis of 2D and 3D cell culture models. Molecules 26 (3), 717. https://doi.org/10.3390/molecules26030717.

Hung, H.-I., Klein, O.J., Peterson, S.W., et al., 2016. PLGA nanoparticle encapsulation reduces toxicity while retaining the therapeutic efficacy of EtNBS-PDT in vitro. Sci Rep. 6 (1), 33234. https://doi.org/10.1038/srep33234.

Ivanova, D., Zhelev, Z., Aoki, I., et al., 2016. Overproduction of reactive oxygen species - obligatory or not for induction of apoptosis by anticancer drugs. Chin. J. Cancer Res. 28 (4), 383–396. https://doi.org/10.21147/j.issn.1000-9604.2016.04.01.

Jabir, N.R., Tabrez, S., Ashraf, G.M., et al., 2012. Nanotechnology-based approaches in anticancer research. Int. J. Nanomed. 7, 4391–4408. https://doi.org/10.2147/ijn.s33838.

Jabir, N.R., Firoz, C.K., Bhushan, A., et al., 2018a. The use of azoles containing natural products in cancer prevention and treatment: an overview. Anticancer Agents Med. Chem. 18 (1), 6–14. https://doi.org/10.2174/1871520616666160520112839.

Jabir, N.R., Islam, M.T., Tabrez, S., et al., 2018b. An insight towards anticancer potential of major coffee constituents. Biofactors 44 (4), 315–326. https://doi.org/10.1002/biof.1437.

Khiewkamrop, P., Surangkul, D., Srikummool, M., et al., 2022. Epigallocatechin gallate triggers apoptosis by suppressing de novo lipogenesis in colorectal carcinoma cells. FEBS Open Bio 12 (5), 937–958. https://doi.org/10.1002/2211-5463.13391.

Lazzari, G., Couvreur, P., Mura, S., 2017. Multicellular tumor spheroids: a relevant 3D model for the in vitro preclinical investigation of polymer nanomedicines. Polym. Chem. 8 (34), 4947–4969. https://doi.org/10.1039/C7PY00559H.

Li, H., Zhang, M., Wang, X., et al., 2022a. Advancements in the treatment of metastatic hormone-sensitive prostate cancer. Front. Oncol. 12,. https://doi.org/10.3389/fonc.2022.913438 913438.

Li, S., Zhao, S., Guo, Y., et al., 2022b. Clinical efficacy and potential mechanisms of acupoint stimulation combined with chemotherapy in combating cancer: A review and prospects. Front. Oncol. 12.

Liu, C., Li, P., Qu, Z., et al., 2019. Advances in the antagonism of epigallocatechin-3-gallate in the treatment of digestive tract tumors. Molecules 24 (9), E1726. https://doi.org/10.3390/molecules24091726.

Lushchak, V.I., 2016. Time-course and intensity-based classifications of oxidative stresses and their potential application in biomedical, comparative and environmental research. Redox Rep. 21 (6), 262–270. https://doi.org/10.1080/13510002.2015.1126940.

Mazurakova, A., Samec, M., Koklesova, L., et al., 2022. Anti-prostate cancer protection and therapy in the framework of predictive, preventive and personalised medicine — comprehensive effects of phytochemicals in primary, secondary and tertiary care. EPMA Journal. 13 (3), 461–486. https://doi.org/10.1007/s13167-022-00288-z.

Michy, T., Massias, T., Bernard, C., et al., 2019. Verteporfin-loaded lipid nanoparticles improve ovarian cancer photodynamic therapy in vitro and in vivo. Cancers 11 (11), E1760. https://doi.org/10.3390/cancers11111760.

Mittal, S., Sharma, P.K., Tiwari, R., et al., 2017. Impaired lysosomal activity mediated autophagic flux disruption by graphite carbon nanofibers induce apoptosis in human lung epithelial cells through oxidative stress and energetic impairment. Part Fibre Toxicol. 14 (1), 15. https://doi.org/10.1186/s12989-017-0194-4.

Oves, M., Aslam, M., Rauf, M., et al., 2018. Antimicrobial and anticancer potential of silver nanoparticles synthesized from trivial Phoenix dactylifera root hair extracts. Mater. Sci. Eng. C 89, 429–443.

Perez, J.E., Nagle, I., Wilhelm, C., 2021. Magnetic molding of tumor spheroids: emerging model for cancer screening. Biofabrication 13, (1). https://doi.org/10.1088/1758-5090/abc670 015018.

Picot, F., Shams, R., Dallaire, F., et al., 2022. Image-guided Raman spectroscopy navigation system to improve transperineal prostate cancer detection. Part 1: Raman spectroscopy fiber-optics system and in situ tissue characterization. J. Biomed. Opt. 27 (9). https://doi.org/10.1117/1.JBO.27.9.095003.

Pinto, B., Henriques, A.C., Silva, P.M.A., et al., 2020. Three-dimensional spheroids as in vitro preclinical models for cancer research. Pharmaceutics. 12 (12), 1186. https://doi.org/10.3390/pharmaceutics12121186.

Porporato, P.E., Filigheddu, N., Pedro, J.-M.-B.-S., et al., 2018. Mitochondrial metabolism and cancer. Cell Res. 28 (3), 265–280. https://doi.org/10.1038/cr.2017.155.

Russo, G.L., Stampone, E., Cervellera, C., et al., 2020. Regulation of p27Kip1 and p57Kip2 functions by natural polyphenols. Biomolecules 10 (9), 1316. https://doi.org/10.3390/biom10091316.

Sayegh, N., Swami, U., Agarwal, N., 2022. Recent advances in the management of metastatic prostate cancer. JCO Oncol. Practice. 18 (1), 45–55. https://doi.org/10.1200/OP.21.00206.

Sims, L.B., Huss, M.K., Frieboes, H.B., et al., 2017. Distribution of PLGA-modified nanoparticles in 3D cell culture models of hypo-vascularized tumor tissue. J. Nanobiotechnol. 15 (1), 67. https://doi.org/10.1186/s12951-017-0298-x.

Sung, H., Ferlay, J., Siegel, R.L., et al., 2021. Global cancer statistics 2020: GLOBOCAN estimates of incidence and mortality worldwide for 36 cancers in 185 countries. CA Cancer J. Clin. 71 (3), 209–249. https://doi.org/10.3322/caac.21660.

Tabrez, S., Priyadarshini, M., Urooj, M., et al., 2013. Cancer chemoprevention by polyphenols and their potential application as nanomedicine. J. Environ. Sci. Health C Environ. Carcinog. Ecotoxicol. Rev. 31 (1), 67–98. https://doi.org/10.1080/10590501.2013.763577.

Zhao, J., Blayney, A., Liu, X., et al., 2021. EGCG binds intrinsically disordered N-terminal domain of p53 and disrupts p53-MDM2 interaction. Nat. Commun. 12 (1), 986. https://doi.org/10.1038/s41467-021-21258-5.